Vol. 14, pp. 199–205 (2017)
doi: 10.2142/biophysico.14.0_199

Biophysics and Physicobiology
https://www.jstage.jst.go.jp/browse/biophysico/

Review Article

Structural basis for the molecular interactions in DNA damage tolerances

Hiroshi Hashimoto[1], Asami Hishiki[1], Kodai Hara[1] and Sotaro Kikuchi[1,2]

[1]*School of Pharmaceutical Sciences, University of Shizuoka, Shizuoka 422-8002, Japan*
[2]*Department of Pharmacology, University of Texas Southwestern Medical Center, Dallas, TX 75390*

Recieved October 3, 2017; accepted November 18, 2017

DNA damage tolerance (DDT) is a cell function to avoid replication arrest by DNA damage during DNA replication. DDT includes two pathways, translesion DNA synthesis (TLS) and template-switched DNA synthesis (TS). DDT is regulated by ubiquitination of proliferating cell nuclear antigen that binds to double-stranded DNA and functions as scaffold protein for DNA metabolism. TLS is transient DNA synthesis using damaged DNA as a template by error-prone DNA polymerases termed TLS polymerases specialized for DNA damage. TS, in which one newly synthesized strand is utilized as an undamaged template for replication by replicative polymerases, is error-free process. Thus, DDT is not inherently a repair pathway. DDT is a mechanism to tolerate DNA damage, giving priority to DNA synthesis and enabling finish of DNA replication for cell survival and genome stability. DDT is associated with cancer development and thus is of great interest in drug discovery for cancer therapy. This review article describes recent progress in structural studies on protein-protein and protein-DNA complexes involved in TLS and TS, providing the molecular mechanisms of interactions in DDT.

Corresponding author: Hiroshi Hashimoto, School of Pharmaceutical Sciences, University of Shizuoka, 52-1 Yada, Suruga-ku, Shizuoka 422-8002, Japan.
e-mail: hash@u-shizuoka-ken.ac.jp

Key words: DNA damage tolerance, translesion DNA synthesis, template-switching, protein-protein interaction, crystal structure

Genomic DNA is constantly damaged by various internal and external factors. In fact, it has been roughly estimated that an individual cell can suffer up to one million DNA damages per day. The majority of DNA lesions stall replicative polymerases, such as DNA polymerase (Pol) δ or Polε, resulting in the arrest of DNA replication. This replication arrest causes lethal effects such as genomic instability and cell-death. To avoid replication arrest by DNA damage and to restart DNA synthesis at damaged site, cells employ DNA damage tolerance (DDT) [1]. DDT is not inherently a repair pathway. DDT is a mechanism to tolerate DNA damage, enabling finish of DNA replication for cell survival and genome stability. DNA damages are repaired by appropriate DNA repair pathways after replication. Thus, DDT is also termed post replication repair. DDT can be divided into two different pathways that continue to synthesize DNA, translesion and template-switched DNA syntheses (Fig. 1). Translesion DNA synthesis (TLS) is transient DNA synthesis using a damaged template by error-prone DNA polymerases specialized for DNA damage. These DNA polymerases are known as TLS polymerases. TLS is an inherently error-prone DNA synthesis. Template-switched DNA synthesis (template-switching, TS), also known as the damage avoidance path-

◀ ***Significance*** ▶

DNA damage tolerance (DDT) is crucial for cell survival and genome stability, although it is not a repair pathway. Paradoxically, DDT is associated with cancer development and thus the molecular interactions involved in DDT could be expected to be a drug target for cancer therapy. Crystal structures of protein-protein and protein-DNA complexes in DDT might provide the structural basis for novel strategy in drug discovery.

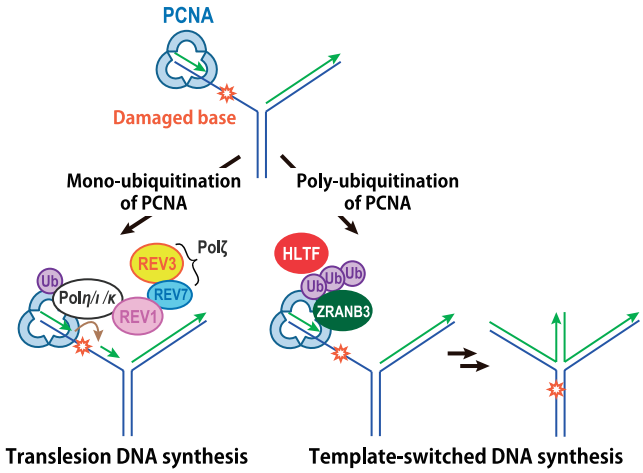

Figure 1 Scheme of DNA damage tolerance pathways. Template and primer strands are shown in blue and green, respectively.

way, in which one newly synthesized strand is utilized as an undamaged template for replication by replicative polymerases, is an error-free process. Several DNA helicases including HLTF and ZRANB3 are crucially engaged in this pathway and these are involved in reversal of the replication fork. HLTF and ZRANB3, might be involved in the early and late stages of the TS, respectively.

TLS and TS pathways in DDT are initiated by the ubiquitination of K164 of proliferating cell nuclear antigen (PCNA), a scaffold protein that binds to double-stranded DNA (dsDNA) and promotes DNA synthesis by DNA polymerases [2]. Mono-ubiquitination of PCNA at K164 by RAD6-RAD18, an E2-E3 ubiquitination complex, stimulates DNA synthesis by TLS polymerases that include REV1, Polη, Polι, Polκ, and Polζ (REV7-REV3 complex) in human. In contrast, poly-ubiquitination of PCNA at K164 promotes TS pathway. The K63-linked poly-ubiquitination of PCNA at K164 is catalyzed by MMS2-UBC13 as E2 ubiquitin conjugating enzyme and RAD5 (HLTF or SHPRH in human) as E3 ubiquitin ligase. DDT is associated with cancer development and thus the molecular interactions to regulate DDT are of great interest in cancer research. In this review article, we describe recent progress in structural studies of protein-protein and protein-DNA complexes involved in DDT and their interactions, providing the molecular mechanisms underlying DDT.

1. Molecular mechanism of polymerase interactions in translesion DNA synthesis

It is generally thought that TLS includes two steps performed by at least two types of TLS polymerase, termed inserter and extender polymerases [3,4]. In the first step, an inserter polymerase classified into Y-family DNA polymerase such as REV1, Polη, Polι, and Polκ [5] incorporates a nucleotide opposite the DNA lesion instead of the stalled replicative polymerase at the damage site. In the second step, the extender polymerase, Polζ composed of REV3 and REV7 subunits, extends additional nucleotides. Then, a replicative polymerase restarts DNA synthesis. In these processes, PCNA functions as a scaffold protein to tether DNA polymerases on dsDNA. In fact, inserter polymerases contain a PCNA binding motif termed PCNA interacting protein box (PIP-box) (Fig. 2a). Structural studies on PCNA in complex with peptides of inserter polymerases revealed the molecular mechanisms to regulate interactions of inserter polymerases with PCNA [6]. Furthermore, structural studies on Polζ and REV1 provided implication for recruitment of extender polymerase and mechanism of polymerase switching [7–13].

1-1. Mechanism to regulate interactions of inserter polymerases with PCNA

PCNA forms a ring-shaped homo trimer and binds dsDNA within the central pore, thereby functioning as a "sliding clamp" on DNA [14,15]. In combination with its DNA binding function, PCNA is now known as a *bona fide* hub protein that physically interacts with more than hundreds of proteins involved in DNA metabolism, including DNA replication, repair, recombination, and sister-chromatid cohesion, and that provides a molecular platform to stimulate the functions of partner proteins [4]. Proteins that interact with PCNA contain PIP-box [16,17]. The consensus sequence of canonical PIP-box is defined as Q-xx-[L/I/M]-xx-[F/Y]-[F/Y], where x is any residue (Fig. 2b). Namely, glutamine, hydrophobic, and two aromatic residues are conserved in the canonical PIP-box at position 1, 4, 7, and 8, respectively (Fig. 2b), and side chains of these residues bind to the outer surface of the ring structure of PCNA (Fig. 2c–e). Polδ, a replicative DNA polymerase, consists of four subunits, p125, p50, p66, and p12 subunits in human. Of these, p66 subunit contains the canonical PIP-box (Fig. 2b). The p66 subunit of Polδ is hereafter simply abbreviated as "Polδ" for clarification, unless otherwise noted. Crystal structure of PCNA in complex with the canonical PIP-box peptide of Polδ is shown in Figure 2d [18]. The side chain of Q456 (position 1) binds to the hydrophilic pocket of PCNA, and I459 (position 4), F461 (position 7), and F463 (position 8) bind to the hydrophobic pockets of PCNA (Fig. 2d, e). Distinct from Polδ, the glutamine residue at position 1 is not conserved in inserter polymerases, Polη, Polι, and Polκ that have non-canonical PIP-boxes (Fig. 2b). In the absence of DNA damage, DNA synthesis by TLS polymerases is not adequate, because TLS is frequently error-prone process. Therefore, binding affinity of non-canonical of PIP-boxes of inserter polymerases for PCNA is supposed to be lower than that of replicative polymerases. Crystal structures of PCNA in complex with the non-canonical PIP-boxes of Polη, Polι, and Polκ revealed a structural basis of low affinity of the non-canonical PIP-boxes for PCNA [6].

Structures of the non-canonical PIP-boxes of inserter

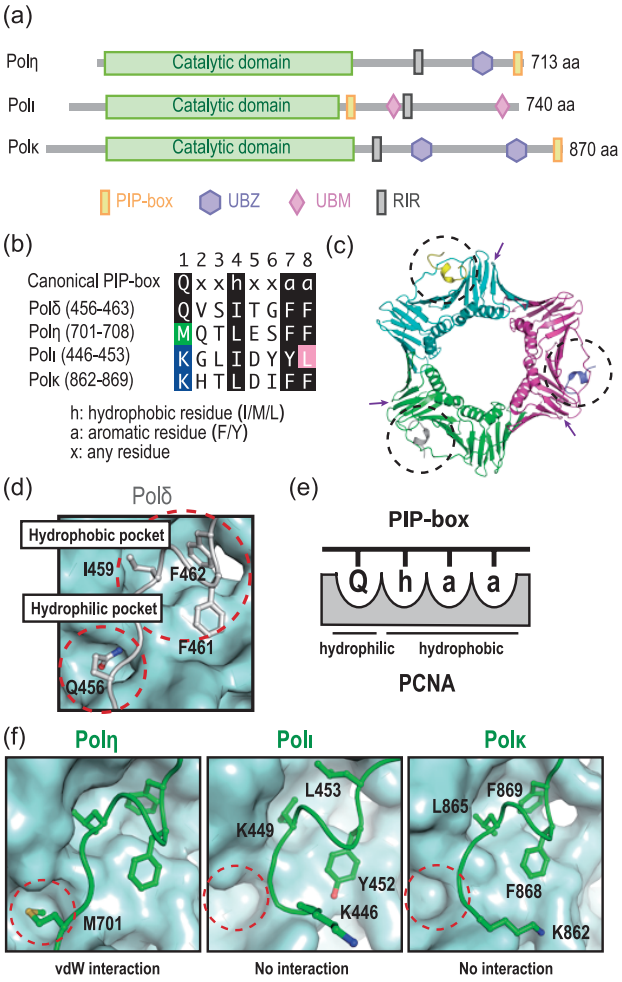

Figure 2 (a) Domain architectures of human Polη, Polι, and Polκ. Polη and Polκ have PIP-box in their C-termini, and Polι has PIP-box in the internal region. Polη has a UBD termed the UBZ domain, which is a CCHH-type Zn-finger domain. Polκ has two UBZ domains, which are CCHC-type Zn-finger domains. Polι has two UBDs termed the UBM domains. Polη, Polι, and Polκ have RIR that has conserved two phenylalanines (FF) similar to PIP-box. (b) Amino acid sequence of the canonical and non-canonical PIP-boxes. Positions of amino acid residues (1~8) are indicated above sequences. Consensus sequence of the canonical PIP-box are shown on the top. Conserved residues are highlighted by black backgrounds. Specific residues of non-canonical PIP-boxes of TLS polymerases are highlighted by green, blue, and pink backgrounds. (c) Overall structure of PCNA in complex with a PIP-box peptide. Crystal structure of human PCNA in complex with Polι peptide is shown as a representative structure of PIP-box bound to PCNA (PDB ID: 2ZVM). PIP-box binding site of PCNA and K164 subjected to ubiquitination in DTT are indicated by dot circles and arrows, respectively. (d) Structure of the canonical PIP-box of Polδ bound to PCNA. Polδ bound to PCNA is shown by silver tube (PDB ID: 1U76). Conserved residues within the canonical PIP-box (Q456, I459, F462, and F463) are shown by stick representation. PCNA is shown by surface representation colored in pale cyan. (e) Schematic drawing of interaction between the canonical PIP-box and PCNA. Residues "h" and "a" correspond to those of (b) (f) Structures of the non-canonical PIP-boxes of Polη, Polι, and Polκ bound to PCNA. Polη (PDB ID: 2ZVK), Polι (PDB ID: 2ZVM), and Polκ (PDB ID: 2ZVL) are shown in the left, center, and right panels, respectively. PCNA is shown by surface representation colored in pale cyan. TLS polymerases are shown by green tube. Residues at positions 1, 4, 7, and 8 are shown by stick representations.

polymerases binding to PCNA are shown in Figure 2f. Interestingly, the side chain of M701 at position 1 of Polη inserts into the hydrophilic pocket of PCNA as observed in the conserved glutamine residue of the canonical PIP-box such as Polδ (Fig. 2f, left panel). The interaction between M701 of Polη and PCNA is van der Waals contact, which could be weaker than electrostatic interactions observed in Q456 of Polδ. Unexpectedly, the lysine residues of Polι and Polκ at position 1 have no contact with the pocket of PCNA (Fig. 2f, center and right panels). M701Q mutant of Polη interacts with PCNA by roughly 4 times stronger than the wild-type of Polη [6], suggesting that the low affinity of inserter polymerases for PCNA might depend on interactions between the residue at position 1 of PIP-box and the hydrophilic pocket of PCNA. In the first step of TLS, a replicative polymerase is replaced with an inserter polymerase. To switch DNA polymerases and facilitate DNA synthesis by inserter polymerases, increase of their affinity for PCNA would be required. As mentioned above, the mono-ubiquitination of PCNA initiates TLS pathway. The ubiquitination of PCNA could increase affinity of inserter polymerases for PCNA. Consistent with this, Polη, Polι, and Polκ contain one or two ubiquitin binding domains, UBM or UBZ (Fig. 2a). Therefore, affinity of inserter polymerases for PCNA might be regulated by the residue at position 1 of PIP-box and the ubiquitination of PCNA.

1-2. Mechanism of recruitment of extender polymerase and polymerase switching

In the second step of TLS, an inserter polymerase is replaced with the extender polymerase, Polζ. As briefly mentioned above, Polζ consists of two subunits, REV3 and REV7 [19,20]. REV3 is the catalytic subunit of Polζ that belongs to B-family DNA polymerase, but lacks 3'–5' exonuclease activity. REV3 can extend a primer strand with terminal mismatches. REV7 is the non-catalytic subunit and interacts with the central region of REV3 [20]. Interestingly, REV7 also interacts with the C-terminal domain of REV1 (REV1-CTD) [21,22]. Furthermore, REV1-CTD interacts with Polη, Polι, and Polκ *via* the REV1-interacting region (RIR) (Fig. 2a) [22]. These interactions are summarized in Figure 3a, implying multiple and dynamic interactions involved in polymerase switching during TLS. Human REV3 is a huge polypeptide chain composed of 3,130 amino acid residues. Therefore, structural and biochemical characterizations of REV3 are still limited owing to the difficulty in preparation of a recombinant REV3 [23]. On the other hand, REV7 is a small polypeptide composed of 211 amino acid residues in human. Recently, REV7 is getting characterized structurally [7, 10–13, 24]. Structural studies on REV7 and REV1-CTD clarified the molecular mechanism of multiple interactions and polymerase switching in TLS [7–13]. In some crystallographic studies on human REV7, the R124A mutation was introduced in REV7 to facilitate crystallization [25].

Structure of human REV7 in complex with a REV3 frag-

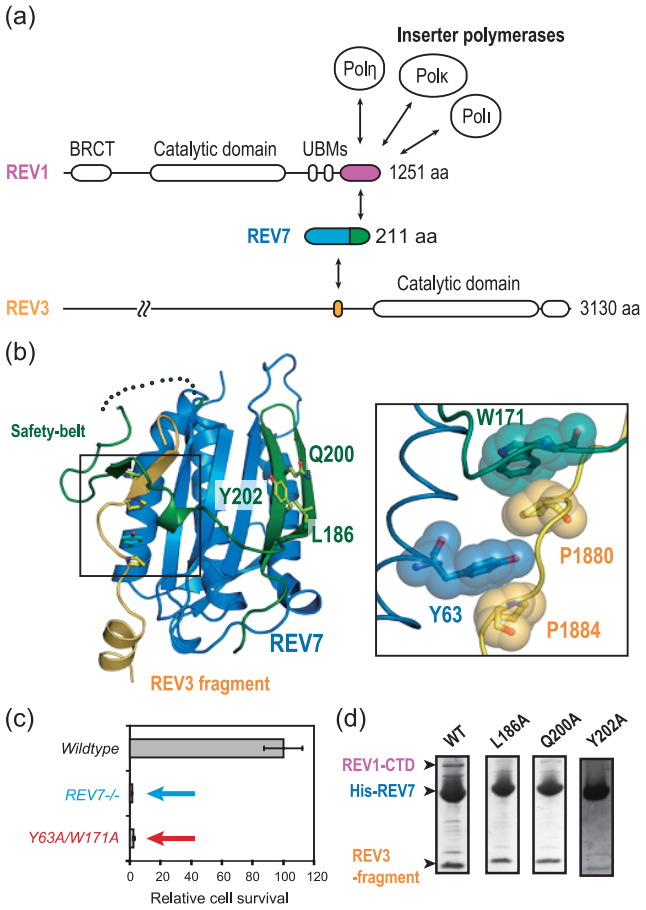

Figure 3 (a) Domain architectures and interactions of human REV1, REV7, and REV3. The C-terminal domain of REV1, REV7, the C-terminal region of REV7 (termed the "safety-belt"), and the REV7-interacting region of REV3 are shown in magenta, blue, green, and yellow, respectively. Double-headed arrows indicate physical interactions. (b) Crystal structure of human REV7 in complex with a REV3 fragment. Structure of human REV7 in complex with a REV3 fragment (residues 1874–1898) is shown by ribbon presentations (PDB ID: 3ABD). A Disordered loop (residues 155–160) are shown by dashed lines. REV7 and REV3 fragment are colored light blue and yellow, respectively. The C-terminal region of REV7 (residues 153–211) corresponding to the safety belt is shown in green. L186, Q200, and Y202 of REV7 responsible for REV1 binding are shown as stick representations. Structural details of interaction between REV7 and REV3 are shown in the right panel. Colors correspond to those in the left panel. Y63 and W171 of REV7, and P1880 and P1884 of REV3 which are responsible for interaction between REV7 and REV3 are shown as stick and transparent CPK representations. (c) Sensitivities of REV7 mutant cells to cisplatin using chicken DT40 cells. Results of rapid survival assays using chicken DT40 *REV7*$^{-/-}$ cells treated with cisplatin are indicated. Relative cell survival of three genotypes, *Wildtype*, *REV7*$^{-/-}$, and *Y63A/W171A*, are shown as bar graphs with standard deviation bars. *Wildtype* and *Y63A/W171A* indicate *REV7*$^{-/-}$ cells artificially overexpressing wildtype *REV7* and *REV7(Y63A/W171A)* mutant, respectively. (d) Binding assays of REV7-REV3 complex with the C-terminal domain of REV1. Recombinant GST-fused REV1 (residues 1130–1251) was incubated with recombinant His-tagged REV7 or REV7 mutant in complex with REV3 fragment (1847–1898) bound to nickel-Sepharose beads. After washing a few times, bound proteins were resolved by SDS-PAGE.

ment is shown in Figure 3b, left panel. REV7 consists of three α-helices, eight β-strands, and 3_{10} helices. The REV3 fragment bound to REV7 comprises a β-strand and an α-helix. Interestingly, the REV3 fragment is wrapped in the C-terminal region of REV7 termed the "safety-belt", resulting in a knot structure. Structural details of interaction between REV7 and REV3 are shown in Figure 3b, right panel. The aromatic rings of Y63 and W171 of REV7 stack with P1884 and P1880 of REV3, respectively. Interaction assay revealed that the Y63A/W171A double mutant of REV7 abolished the binding to REV3 [7]. Furthermore, cell function of the interaction was revealed by survival assay using chicken DT40 bursal lymphoma cells under cisplatin exposure. Cisplatin is a DNA-damaging agent that produces variety of cross-linked DNA, thereby showing cytotoxic effect, and thus it widely used in chemotherapy of tumor. Consistent with a previous study [26], the REV7 deficient (*REV7*$^{-/-}$) DT40 cells showed low survival rate (Fig. 3c, middle bar) compared with *REV7*$^{-/-}$ cells artificially overexpressing wild type REV7 (Fig. 3c, top bar), indicating extreme sensitivity to cisplatin. Remarkably, *REV7*$^{-/-}$ cells overexpressing REV7(Y63A/W171A) mutant also showed extreme sensitivity (Fig. 3c, bottom bar). These results definitively indicate that REV7-REV3 interaction has an important role in TLS. In other words, these suggest that the interaction is crucial for cisplatin resistance in cancer cells. Thus, interactions between REV7 and REV3 might be the attractive target to develop anticancer drugs.

REV7 interacts with not only REV3, but also the C-terminal region of REV1 (Fig. 3a) [21,22]. Exhaustive *in vitro* binding assay using numerous alanine mutants of REV7 firstly confirmed a formation of ternary complex of REV1-REV7-REV3 and reveled that L186, Q200, and Y202 are crucial for REV1 binding (Fig. 3d) [7]. Intriguingly, these residues located on the C-terminal β-strands of REV7 (Fig. 3b). Because of the REV3 binding resulting in a knot structure, the C-terminal region of REV7could be intrinsically disordered without the REV3 binding, implying a sequential binding of REV7, REV3, and REV1. Subsequently, crystal structures of protein complexes including REV1-CTD revealed details of REV7-REV1 interaction and provided structural basis for polymerase switching [8–13]. The interactions between REV1 and REV7-REV3 complex revealed by crystal structures were consistent with previous biochemical results [7,10,11]. Namely, L186 of REV7 binds to the hydrophobic pocket formed by L1203, Y1244, and L1248 of REV1, and these van der Waals contacts were essential for the interaction between REV7 and REV1. Y202 and Q200 of REV7 are also significantly involved in the interaction in hydrophobic and hydrophilic manners, respectively (Fig. 4a) [11]. As descried above, REV1-CTD binds the inserter polymerases such as Polη, Polι, and Polκ (Fig. 1) [22]. Structural studies revealed that the inserter binding site of REV1 was not overlapped with the REV7 binding site [8, 9], enabling the formation of an inserter-extender complex (Fig. 4b) [10].

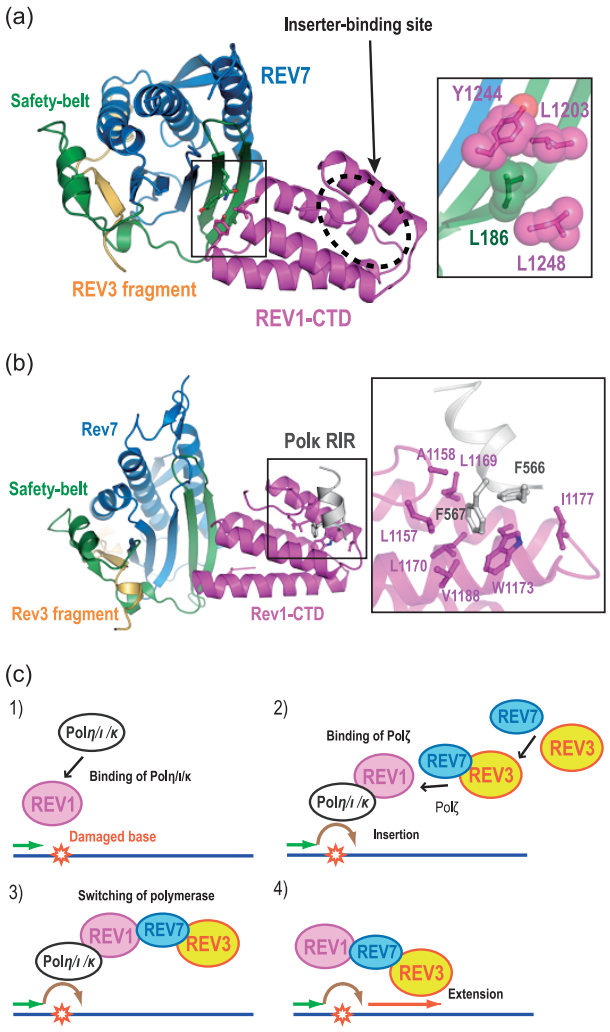

Figure 4 (a) Crystal structure of the ternary complex of REV1-REV7-REV3. Structure of the ternary complex is shown by ribbon representation (PDB ID: 3VU7). Colors of REV7 and REV3 correspond to those of Figure 2a. The C-terminal domain of REV1 (REV1-CTD) is shown in magenta. Structural details of interaction between REV7 and REV1 are shown in the right panel. Residues responsible for REV7-REV1 interaction are shown by stick and transparent CPK representations. (b) Crystal structure of the quaternary complex. Structure of the quaternary complex composed of mouse Rev1, Rev7, Rev3, and Polκ is shown by ribbon representation (PDB ID: 4FJO). Polκ RIR peptide is colored grey. (c) Schematic model of polymerase switching. Template, primer, and extended strands are shown in blue, green, and orange, respectively.

Polκ RIR adopted a helical conformation. Two phenylalanines (F565 and F566) conserved within RIRs of inserter polymerases are accommodated into a hydrophobic cleft of mouse Rev1, an ortholog of human REV1, *via* van der Waals contacts with L1157, A1158, L1169, L1170, W1173, I1177, and V1188. Based on these results, the mechanism of polymerase switching might be proposed, as follows (Fig. 4c). REV1 localizes on DNA damaged site through the interaction with RAD18 [27], an E3 ubiquitin ligase for PCNA, and REV1-CTD provides a scaffold to recruit other inserters such as Polη, Polι, and Polκ. The inserter-REV1 complex facilitates to insert a nucleotide on damaged site. The extender polymerase, Polζ consisting of REV7 and REV3, is recruited on the primer end through the interaction between REV1 and REV7. Formation of a quaternary complex consisting of an inserter and extender mediated by REV1-CTD facilitates switching from an inserter to the extender polymerases and then Polζ extends a few additional nucleotides. After that, a replicative polymerase restarts DNA replication.

2. Mechanism of an early step in TS

DDT includes two pathways, TLS and TS, but how one pathway is chosen over the other remains a mystery. TLS appears to be a rapid process, because it is performed by several TLS polymerases and does not require structural change of the replication fork. In contrast, TS is a much more complicated process including regression of the stalled replication fork, DNA synthesis using switched template, and reversal of the regressed fork (Fig. 1). Recently, a mechanism of an early step in TS is getting clarified by structural studies on HLTF, a crucial protein that has activities of E3 ubiquitin ligase and DNA helicase [28–30]. The domain architecture of human HLTF is shown in Figure 5a. Previously, a bioinformatics has suggested that the N-terminal HIRAN domain of HLTF has DNA binding activity [31]. The crystal structure of the HIRAN domain of human HLTF in complex with dsDNA revealed the DNA recognition mechanism of HLTF in an early step of TS [28].

The HIRAN domain of HLTF adopts a β-barrel structure composed of six β-strands flanked with two α-helices (Fig. 5b), resulting in an OB-fold structure that contains oligonucleotide-binding proteins. HLTF HIRAN domain has a concave surface that interacts with the two bases of the primer stand of dsDNA. Interestingly, the 3'-end of the primer strand is specifically bound to a pocket of the domain. Structural details of interaction between HLTF HIRAN domain and DNA is shown in Figure 5b, left panel. D94 of HLTF recognizes 3'-OH of primer strand and it binds to DNA so that it unwinds the dsDNA by two tyrosine residues (Y72 and Y93) that pinch two bases of 3'-end of the primer strand (Cyt12 and Cyt13). Based on the structure, a mechanism of an early step in TS is proposed, as follows (Fig. 5b). HLTF binds to the 3'end of the primer strand of the stalled replication fork through the interaction between the HIRAN domain and DNA. HLTF and RAD18 could perform poly-ubiquitination of K164 of PCNA, whereas the mechanism underlying poly-ubiquitination of PCNA by RAD18 and HLTF is controversial [32,33]. The poly-ubiquitinated PCNA could be recognized by ZRANB3, a DNA helicase that contains two PCNA-binding motifs and a poly-ubiquitin binding domain, thereby ZRANB3 might be recruited to the damaged site and the fork regression to switch template strand might be facilitated.

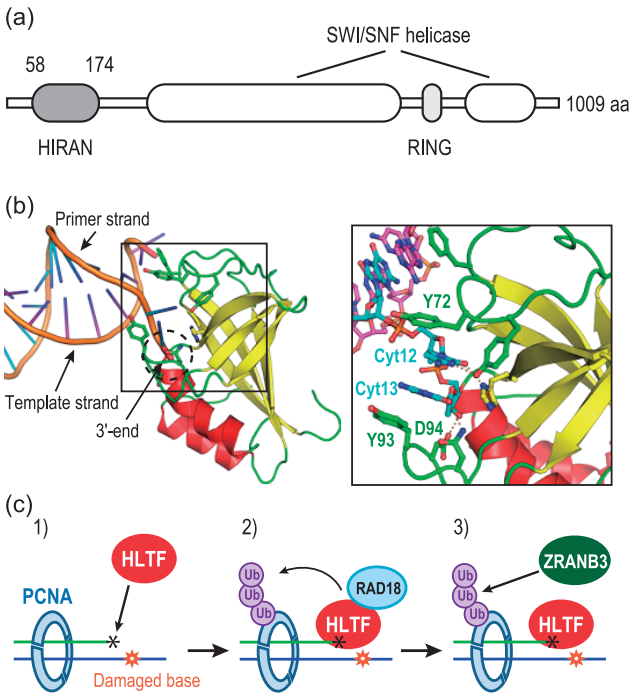

Figure 5 (a) Domain architecture of human HLTF. HLTF consists of HIRAN, SWI/SNF helicase and E3 RING domains. The helicase domain is divided to N- and C-terminal parts by insertion of the RING domain. (b) Crystal structure of the HIRAN domain of HLTF in complex with dsDNA. HIRAN domain and DNA are shown by ribbon and stick representations, respectively (PDB ID: 4XZF). Structural details of interaction between the HIRAN domain and DNA are shown in the right panel. Electrostatic interactions are shown by dots. (c) Schematic model of an initial step in template-switching. Template and primer strands are shown in blue and green, respectively. Asterisk indicates the 3'-terminal end of primer strand. Ubiquitin chain is shown by purple bubbles.

3. Perspectives

In this review, we described crystal structures of protein-protein and protein-DNA complexes crucially involved in DDT and their interactions, thereby providing molecular mechanisms. Crystal structures of PCNA in complex with Polη, Polι, and Polκ peptides clarified details of their interactions, whereas interactions between REV1 and PCNA remain unclear. It is considered that REV1 does not have PIP-box. Instead, the N-terminal BRCT domain of REV1 [34,35] and the C-terminal region of central polymerase domain [36] independently interact with PCNA. However, structural details of the interaction between REV1 and PCNA are unclear. Therefore, structural study of PCNA-REV1 complex is strongly required to clarify the interaction and more detailed mechanism underlying polymerase-switching. Recent study identified additional PIP-boxes of Polη and Polκ, and revealed redundant and additive functions of multiple PIP-boxes and UBZs of Polη in enhancing cell survival after UV irradiation [37]. That implies orchestrated interactions by TLS polymerases and PCNA *in vivo*. To address the mechanism behind orchestration of TLS polymerases, structural studies of a full-length TLS polymerase and mono-ubiquitinated PCNA are required. Recently, low resolution structures of Polη and mono-ubiquitinated PCNA by electron microscopy revealed domain arrangements in their complex bound to DNA [38]. To date, many structures of catalytic domain of inserter polymerases have revealed structural basis for the mechanisms of nucleotide insertion at atomic resolution. In contrast, structural information about the extender, Polζ, is very limited in an overall structure of yeast Polζ by electron microscopy at low resolution [39]. High resolution structures of Polζ and its DNA complex are needed to resolve the molecular mechanism of the extension step in TLS.

Structural studies on the HIRAN domain of HLTF have shed light on the mechanisms of an early step of TS in which the HIRAN domains could be involved. But, structural detail of the molecular mechanism behind overall TS pathway is still an open question. Very recently, a structural study on ZRANB3 provided basis for functions as a structure-specific DNA nuclease and PCNA interactions [40]. However, a function as DNA helicase remains unclear. Further structural and biochemical studies on HLTF and ZRANB3 are urgently required to address challenges accompanying TS.

Conflict of Interest

The authors declare no conflict of interests.

Author Contributions

H. H., A. H., K. H., and S. K. drafted the manuscript and prepared figure representations.

References

[1] Branzei, D. & Psakhye, I. DNA damage tolerance. *Curr. Opin. Cell. Biol.* **40**, 137–144 (2016).
[2] Stelter, P. & Ulrich, H. D. Control of spontaneous and damage-induced mutagenesis by SUMO and ubiquitin conjugation. *Nature* **425**,188–191 (2003).
[3] Friedberg, E. C., Lehmann, A. R. & Fuchs, R. P. Trading places: how do DNA polymerases switch during translesion DNA synthesis? *Mol. Cell* **18**, 499–505 (2005).
[4] Moldovan, G. L., Pfander, B. & Jentsch, S. PCNA, the maestro of the replication fork. *Cell* **129**, 665–679 (2007).
[5] Ohmori, H., Friedberg, E. C., Fuchs, R. P., Goodman, M. F., Hanaoka, F., Hinkle, D., *et al.* The Y-family of DNA polymerases. *Mol. Cell* **8**, 7–8 (2001).
[6] Hishiki, A., Hashimoto, H., Hanafusa, T., Kamei, K., Ohashi, E., Shimizu, T., *et al.* Structural basis for novel interactions between human translesion synthesis polymerases and proliferating cell nuclear antigen. *J. Biol. Chem.* **284**, 10552–10560 (2009).
[7] Hara, K., Hashimoto, H., Murakumo, Y., Kobayashi, S., Kogame, T., Unzai, S., *et al.* Crystal structure of human REV7 in complex with a human REV3 fragment and structural implication of the interaction between DNA polymerase zeta and REV1. *J. Biol. Chem.* **285**, 12299–12307 (2010).
[8] Pozhidaeva, A., Pustovalova, Y., D'Souza, S., Bezsonova, I.,

Walker, G. C. & Korzhnev, D. M. NMR structure and dynamics of the C-terminal domain from human Rev1 and its complex with Rev1 interacting region of DNA polymerase η. *Biochemistry* **51**, 5506–5520 (2012).
[9] Wojtaszek, J., Liu, J., D'Souza, S., Wang, S., Xue, Y., Walker, G. C., *et al.* Multifaceted recognition of vertebrate Rev1 by translesion polymerases ζ and κ. *J. Biol. Chem.* **287**, 26400–26408 (2012).
[10] Wojtaszek, J., Lee, C. J., D'Souza, S., Minesinger, B., Kim, H., D'Andrea, A. D., *et al.* Structural basis of Rev1-mediated assembly of a quaternary vertebrate translesion polymerase complex consisting of Rev1, heterodimeric polymerase (Pol) ζ, and Pol κ. *J. Biol. Chem.* **287**, 33836–33846 (2012).
[11] Kikuchi, S., Hara, K., Shimizu, T., Sato, M. & Hashimoto, H. Structural basis of recruitment of DNA polymerase ζ by interaction between REV1 and REV7 proteins. *J. Biol. Chem.* **287**, 33847–33852 (2012).
[12] Xie, W., Yang, X., Xu, M. & Jiang, T. Structural insights into the assembly of human translesion polymerase complexes. *Protein Cell* **3**, 864–874 (2012).
[13] Liu, D., Ryu, K. S., Ko, J., Sun, D., Lim, K., Lee, J. O., *et al.* Insights into the regulation of human Rev1 for translesion synthesis polymerases revealed by the structural studies on its polymerase-interacting domain. *J. Mol. Cell. Biol.* **5**, 204–206 (2013).
[14] McNally, R., Bowman, G. D., Goedken, E. R., O'Donnell, M. & Kuriyan, J. Analysis of the role of PCNA-DNA contacts during clamp loading. *BMC Struct. Biol.* **10**, 3 (2010).
[15] De March, M., Merino, N., Barrera-Vilarmau, S., Crehuet, R., Onesti, S., Blanco, F. J., *et al.* Structural basis of human PCNA sliding on DNA. *Nat. Commun.* **8**, 13935 (2017).
[16] Warbrick, E., Lane, D. P., Glover, D. M. & Cox, L. S. A small peptide inhibitor of DNA replication defines the site of interaction between the cyclin-dependent kinase inhibitor p21WAF1 and proliferating cell nuclear antigen. *Curr. Biol.* **5**, 275–282 (1995).
[17] Warbrick, E. PCNA binding through a conserved motif. *Bioessays* **20**, 195–199 (1998).
[18] Bruning, J. B. & Shamoo, Y. Structural and thermodynamic analysis of human PCNA with peptides derived from DNA polymerase-delta p66 subunit and flap endonuclease-1. *Structure* **12**, 2209–2219 (2004).
[19] Nelson, J. R., Lawrence, C. W. & Hinkle, D. C. Thymine-thymine dimer bypass by yeast DNA polymerase zeta. *Science* **272**, 1646–1649 (1996).
[20] Murakumo, Y., Roth, T., Ishii, H., Rasio, D., Numata, S., Croce, C. M., *et al.* A human REV7 homolog that interacts with the polymerase zeta catalytic subunit hREV3 and the spindle assembly checkpoint protein hMAD2. *J. Biol. Chem.* **275**, 4391–4397 (2000).
[21] Murakumo, Y., Ogura, Y., Ishii, H., Numata, S., Ichihara, M., Croce, C. M., *et al.* Interactions in the error-prone postreplication repair proteins hREV1, hREV3, and hREV7. *J. Biol. Chem.* **276**, 35644–35651 (2001).
[22] Ohashi, E., Murakumo, Y., Kanjo, N., Akagi, J., Masutani, C., Hanaoka, F., *et al.* Interaction of hREV1 with three human Y-family DNA polymerases. *Genes Cells* **9**, 523–531 (2004).
[23] Lee, Y. S., Gregory, M. T. & Yang, W. Human Polζ purified with accessory subunits is active in translesion DNA synthesis and complements Polη in cisplatin bypass. *Proc. Natl. Acad. Sci. USA* **111**, 2954–2959 (2014).
[24] Hara, K., Taharazako, S., Ikeda, M., Fujita, H., Mikami, Y., Kikuchi, S., *et al.* Dynamic feature of mitotic arrest deficient 2-like protein 2 (MAD2L2) and structural basis for its interaction with chromosome alignment maintaining phosphoprotein (CAMP). *J. Biol. Chem.* **292**, 17658–17667 (2017).
[25] Hara, K., Shimizu, T., Unzai, S., Akashi, S., Sato, M. & Hashimoto, H. Purification, crystallization and initial X-ray diffraction study of human REV7 in complex with a REV3 fragment. *Acta Crystallogr. Sect. F Struct. Biol. Cryst. Commun.* **65**, 1302–1305 (2009).
[26] Okada, T., Sonoda, E., Yoshimura, M., Kawano, Y., Saya, H., Kohzaki, M., *et al.* Multiple roles of vertebrate REV genes in DNA repair and recombination. *Mol. Cell Biol.* **25**, 6103–6111 (2005).
[27] Wang, Z., Huang, M., Ma, X., Li, H., Tang, T. & Guo, C. REV1 promotes PCNA monoubiquitylation through interacting with ubiquitylated RAD18. *J. Cell Sci.* **129**, 1223–1233 (2016).
[28] Hishiki, A., Hara, K., Ikegaya, Y., Yokoyama, H., Shimizu, T., Sato, M., *et al.* Structure of a Novel DNA-binding Domain of Helicase-like Transcription Factor (HLTF) and Its Functional Implication in DNA Damage Tolerance. *J. Biol. Chem.* **290**, 13215–13223 (2015).
[29] Kile, A. C., Chavez, D. A., Bacal, J., Eldirany, S., Korzhnev, D. M., Bezsonova, I., *et al.* HLTF's Ancient HIRAN Domain Binds 3' DNA Ends to Drive Replication Fork Reversal. *Mol. Cell* **58**, 1090–1100 (2015).
[30] Achar, Y. J., Balogh, D., Neculai, D., Juhasz, S., Morocz, M., Gali, H., *et al.* Human HLTF mediates postreplication repair by its HIRAN domain-dependent replication fork remodelling. *Nucleic Acid Res.* **43**, 10277–10291 (2015).
[31] Iyer, L. M., Babu, M. M. & Aravind, L. The HIRAN domain and recruitment of chromatin remodeling and repair activities to damaged DNA. *Cell Cycle* **5**, 775–782 (2006).
[32] Parker, J. L. & Ulrich, H. D. Mechanistic analysis of PCNA poly-ubiquitylation by the ubiquitin protein ligases Rad18 and Rad5. *EMBO J.* **28**, 3657–3666 (2009).
[33] Masuda, Y., Suzuki, M., Kawai, H., Hishiki, A., Hashimoto, H., Masutani, C., *et al. En bloc* transfer of polyubiquitin chains to PCNA in vitro is mediated by two different human E2–E3 pairs. *Nucleic Acids Res.* **40**, 10394–10407 (2012).
[34] Guo, C., Sonoda, E., Tang, T. S., Parker, J. L., Bielen, A. B., Takeda, S., *et al.* REV1 protein interacts with PCNA: significance of the REV1 BRCT domain in vitro and in vivo. *Mol. Cell* **23**, 265–271 (2006).
[35] Pustovalova, Y., Maciejewski, M. W. & Korzhnev, D. M. NMR mapping of PCNA interaction with translesion synthesis DNA polymerase Rev1 mediated by Rev1-BRCT domain. *J. Mol. Biol.* **425**, 3091–3105 (2013).
[36] Sharma, N. M., Kochenova, O. V. & Shcherbakova, P. V. The non-canonical protein binding site at the monomer-monomer interface of yeast proliferating cell nuclear antigen (PCNA) regulates the Rev1-PCNA interaction and Polζ/Rev1-dependent translesion DNA synthesis. *J. Biol. Chem.* **286**, 33557–33566 (2011).
[37] Masuda, Y., Kanao, R., Kaji., K., Ohmori, H., Hanaoka, F. & Masutani, C. Different types of interaction between PCNA and PIP boxes contribute to distinct cellular functions of Y-family DNA polymerases. *Nucleic Acids Res.* **43**, 7898–7910 (2015).
[38] Lau, W. C., Li, Y., Zhang, Q. & Huen, M. S. Molecular architecture of the Ub-PCNA/Pol η complex bound to DNA. *Sci. Rep.* **5**, 15759 (2015).
[39] Gómez-Llorente, Y., Malik, R., Jain, R., Choudhury, J. R., Johnson, R. E., Prakash, L., *et al.* The architecture of yeast DNA polymerase ζ. *Cell Rep.* **5**, 79–86 (2013).
[40] Sebesta, M., Cooper, C. D. O., Ariza, A., Carnie, C. J. & Ahel, D. Structural insights into the function of ZRANB3 in replication stress response. *Nat. Commun.* **8**, 15847 (2017).